Physica B 684 (2024) 415965

Contents lists available at ScienceDirect

Physica B: Condensed Matter

journal homepage: www.elsevier.com/locate/physb

On the temperature dependence of the current conduction mode in non-homogeneous Pt/*n*-GaN Schottky barrier diode

Mohammed Mamor [a,c,*], Khalid Bouziane [b], Hind Chakir [a,b], Pierre Ruterana [c]

[a] Laboratoire Physique Fondamentale et Appliquée–Safi (LPFA-Safi), Faculté Poly-Disciplinaire, B. P. 4162 Safi, Université Cadi Ayyad, Marrakech, Morocco
[b] LERMA, Collège Ingénierie et Architecture, Université Internationale de Rabat, Parc Technopoles Rabat-Shore, 11100, Sala El Jadida, Morocco
[c] CIMAP, UMR 6252, CNRS, ENSICAEN, Université de Caen-Normandie, CEA, 6 Boulevard du Maréchal Juin, 1400, Caen, France

ARTICLE INFO

Keywords:
Barrier height inhomogeneities
Gaussian distribution of barrier height
Temperature dependence of barrier height
Conduction mode in Pt/*n*-GaN contacts
Thermionic emission theory
Thermionic field emission theory

ABSTRACT

Forward current-voltage (*I–V*) measurements of Pt/*n*-GaN Schottky barrier diode (SBD) are investigated in a wide temperature range (80–400 K). The temperature dependence of the effective Schottky barrier height (SBH) and ideality factor are analyzed on the basis of the thermionic emission (*TE*) model by considering a double Gaussian distribution (DGD) of SBH due to the presence of barrier height inhomogeneities at the Pt/*n*-GaN interface. In the high temperature (HT) region (200–400 K), Pt/*n*-GaN SBD exhibits nearly an ideal behavior in accordance with the *TE* conduction mode. The obtained values of the homogeneous SBH $\overline{\Phi}_{0bn} = 1.33$ eV and Richardson constant $A^{*}_{HT} = 26.86$ A cm^{-2} K^{-2}are in agreement with the theoretical values for *n*-type GaN. In the low temperature (LT) region (80–160 K), the corresponding values $\overline{\Phi}_{0bn} = 0.94$ eV and $A^{*}_{LT} = 14.74$ A cm^{-2} K^{-2} deduced within the *TE* mode deviate strongly from the ideal behavior. This deviation is further confirmed by the large ideality factor. In this work, we provide a strong evidence that the tunneling current including thermionic field emission (*TFE*) largely dominates the conduction mode at low temperature.

1. Introduction

GaN and its related alloys have attracted much interest over the past decade due to their potential application in the field of semiconductor devices [1,2]. For instance, GaN semiconductor has promising physical features for the development of GaN-based high power, high speed and high frequency electronic devices such as the field effect transistors (MESFETs) [1,2], and high electron mobility transistors (HEMTs) [3–5]. The most popular examples of GaN-based applications include blue and ultraviolet (UV) light-emitting diodes (LEDs) [6]. In particular, GaN-based Schottky barrier diodes (SBD) have been used as a component for the above electronic and optoelectronic devices. In this respect, high quality ohmic and Schottky contacts are required. Therefore, a deep understanding of the electrical characteristics of metal (M)/GaN contacts is of fundamental and technological importance for developing GaN based-electronic and optoelectronic devices [7–13]. To this end, several challenges should be addressed in order to have M/GaN devices characterized with high Schottky barrier height (SBH), an ideality factor (n) close to unity and a low reverse current. Effectively, the low Schottky barrier height induces excess current through M/GaN SBD in both forward and reverse characteristics that strongly affects the SBD performances. The thermionic emission (*TE*) model is usually used to extract the Schottky parameters (barrier height and ideality factor), using current-voltage (*I–V*) measurements. The extracted values often exhibit an abnormal temperature dependence. This is reflected by the increase of the barrier height and the decrease of the ideality factor with increasing temperature. This abnormal behavior has been analyzed on the basis of the *TE* model by taking into account the presence of the barrier height inhomogeneities (*BH*i) located at the metal/semiconductor (M/Sc) interface [14–27]. Actually, several models have been developed to describe the *BH*i at M/Sc interface [28–30]. The model developed by Werner and Güttler [28] considers a Gaussian distribution (GD) of SBH with a standard deviation (σ_s) around mean barrier height ($\overline{\Phi}_{bn}$) value. In the latter model, the effective SBH is shown to be both temperature and bias dependent.

Besides the above abnormal features observed in previous reports [16–20], a double Gaussian distribution (DGD) of a non-homogeneous M/Sc Schottky contacts has also been reported. Such DGD is

* Corresponding author. Laboratoire Physique Fondamentale et Appliquée–Safi (LPFA-Safi), Faculté Poly-Disciplinaire, B. P. 4162 Safi, Université Cadi Ayyad, Marrakech, Morocco.
E-mail addresses: mohammedmamor@yahoo.om, m.mamor@uca.ac.ma (M. Mamor).

https://doi.org/10.1016/j.physb.2024.415965
Received 22 February 2024; Received in revised form 24 March 2024; Accepted 12 April 2024
Available online 12 April 2024
0921-4526/

associated with low (LT) and high (HT) temperature regimes, respectively. Among other important electrical parameters, Richardson constant (A^*) is found to be strongly affected by the presence of *BH*i. This is especially true for the Richardson constant at low temperature regime (A^*_{LT}). For instance, Huan et *al* [16] and Yildirim et *al* [18] have assumed the existence of DGD of the barrier heights in Pt/*n*-4H–SiC and Ni/*n*--GaN, respectively. In the low temperature region, the extracted Richardson constant ($A^*_{LT} = 37.4$ A.cm^{-2}K^{-2}) for Pt/*n*-4H–SiC is found to be much lower than the theoretical value (146 A cm^{-2}K^{-2}) [31,32], by contrast to the corresponding high temperature region extracted value $A^*_{HT} = 148.5$ A.cm^{-2}K^{-2} [16]. Ni/*n*-GaN system exhibits also a DGD of SBH in the temperature regions of 80–180 K and 200–400 K [18] with respective values of $A^* = 80$ and 85 A cm^{-2} K^{-2}. On the other hand, Kumar et *al* [19] have reported deduced A* values for Ni/*n*-GaN of 48 A cm^{-2}K^{-2} in 100–200 K range, and 29.2 A cm^{-2}K^{-2} in 200–380 K range. Reddy et *al* [33] investigated the electrical properties of Ru/Pt/n-GaN in the temperature region of 100–420 K. By assuming a DGD, they reported, $A^*_{LT} = 10.29$ A.cm^{-2}K^{-2} and $A^*_{HT} = 27.83$ A.cm^{-2}K^{-2}. Furthermore, Iucolano et *al* [34] and Zhou et *al* [35] have performed measurements on Pt/*n*-GaN system at high temperature regime only (300–450K) and (298–473 K), respectively. They obtained a single GD associated with high temperature A^*_{HT} value of 25 and 35 A cm^{-2}K^{-2}, respectively. The above mentioned results indicate clearly a strong discrepancy in the deduced values of A^*. It is worth to mention that Pt-GaN system shows a very good rectifying characteristics with A^* at HT close to the theoretical value (26.9 A cm^{-2}K^{-2}) [36]. This makes it an ideal candidate for exploring further this discrepancy in the reported results. A systematic investigation of the temperature dependence of the electrical characteristics of Pt/*n*-GaN SBD over a wide temperature range should enable exploring the conduction modes, especially associated with the observed abnormal feature in the low temperature regime.

In this work, the temperature dependent forward current-voltage (*I–V*) characteristics were used to analyze the *BH*i at Pt/*n*-GaN SBD. The observed anomalies in the current-voltage characteristics were analyzed using the potential fluctuation model with two Gaussian distributions of barrier heights. In particular, the values of A^*_{LT} and A^*_{HT} deduced from the DGD of the barrier height are discussed in terms of current conduction modes at Pt/*n*-GaN SBD. We show that *TE* model describes properly the current transport mechanism in the HT regime, while the thermionic field emission (*TFE*) governs the current transport at LT regime in Pt/*n*-GaN SBD.

2. Experimental details

n-type GaN epitaxial layers with a free carrier density of (2–3) × 10^{17} cm^{-3} and a thickness of about 1200 nm, was grown on (0001) Al_2O_3*c*-plane substrate using the metal organic chemical vapor deposition (MOCVD) technique. A low resistance ohmic contact was formed prior SBD fabrication by electron beam deposition of Ti/Al/Ni/Au on the front side of the GaN epilayer, and subsequent annealing at 500 °C for 5 min in a high purity Ar atmosphere was performed [16]. Prior to Schottky contact deposition, the samples were degreased and dipped in an HCl: H2O (1:1) solution. Circular Pt Schottky contacts 0.66 mm in diameter and 120 nm in thickness were fabricated on the *n*-GaN epitaxial layers through a metal contact mask by electron beam deposition. A schematic three-dimensional structure of the fabricated Pt/n-GaN device is displayed in Fig. 1(a), and the energy band diagram of Pt/n-GaN contacts is shown in Fig. 1 (b).

Temperature-dependent *I –V* measurements on Pt/*n*-GaN SBDs were carried out in the range 80–400 K. The details of the SBD fabrication and *I–V* measurement have been reported elsewhere [20].

3. Results and discussion

3.1. Investigation of electrical parameters based on the thermionic emission conduction model

Fig. 2 displays the semi-logarithmic plot of the forward current–voltage measurements of Pt/*n*-GaN SBD as a function of temperature ranging between 80 and 400 K. It shows that the forward ln (*I*)–*V* curve exhibits a linear behavior over a large applied forward voltage range for the considered temperature region. Moreover, the current increases with increasing temperature as predicted by the thermionic emission model regardless of the applied voltage considered.

In the framework of thermionic emission, the current through a SBD can be expressed as [37]:

$$I = I_s \left[\exp\left(\frac{q(V - R_s I)}{n k_B T} \right) - 1 \right] \tag{1a}$$

where n is the ideality factor, R_s the series resistance, V_F the applied forward voltage and I_s the saturation current given by:

$$I_S = A^* S T^2 \exp\left(-\frac{\Phi_{0bn}}{k_B T} \right) \tag{1b}$$

where Φ_{0bn} is the effective barrier height at zero bias, A^* the modified

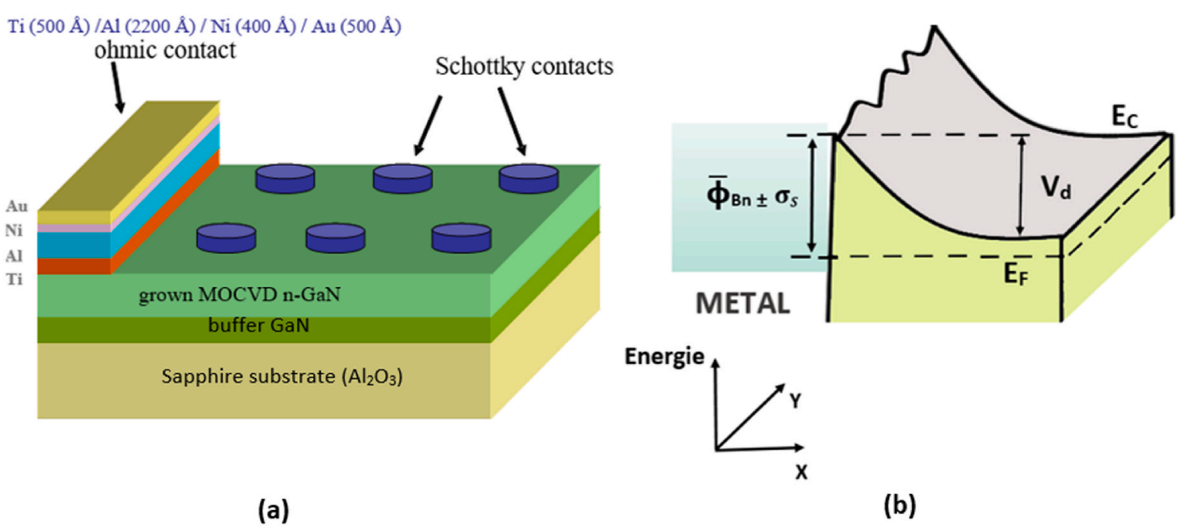

Fig. 1. (a) A Schematic cross section view of Pt/*n*-GaN SBD. (b) A schematic energy band diagram of Pt/*n*-GaN SBD (not to scale).

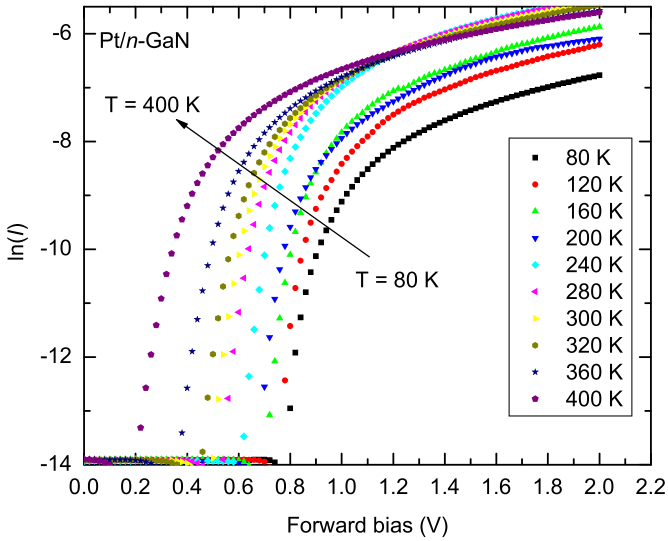

Fig. 2. Experimental forward *I–V* curves of Pt/*n*-GaN SBD measured at different temperatures.

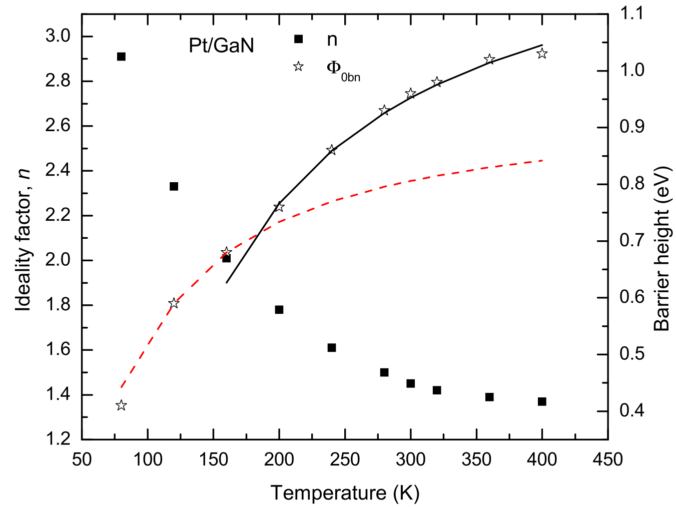

Fig. 3. Deduced effective barrier heights Φ_{0bn} and ideality factor *n* as a function of temperature for Pt/*n*-GaN SBD. Broken and solid lines are for the calculated SBHs using equation (3) for two Gaussian distributions of SBHs in LT region (80–160 K) and HT region (200–400 K), respectively.

Richardson constant with a corresponding theoretical value of 26.9 A cm^{-2} K^{-2} for M/*n*-type GaN Schottky contacts [36], *S* the area of the diode, *T* the temperature and k_B the Boltzmann constant. The series resistance R_s was determined using the Werner method [38], while the ideality factor, *n* as defined in equation (1) was deduced from the slope of the semi logarithmic *I–V* characteristics.

$$n = \frac{q}{k_B T}\frac{dV}{d(\ln I)} \tag{2}$$

The respective experimental values of Φ_{0bn} and *n* were obtained from the fitting of the semi logarithmic *I–V* curve using equations (1) and (2). Their temperature dependence is displayed in Table I (and plotted in Fig. 3). The two Schottky parameters, Φ_{0bn} and *n* exhibit strong temperature dependence, namely Φ_{0bn} increases and *n* decreases with increasing temperature. As mentioned above, Werner method [38] was used to determine the series resistance of the structure and its temperature dependence is also presented in Table I. The series resistance increases with increasing temperature as is expected for semiconductors in the temperature region where there is no freezing out of carriers. The abnormal temperature dependence of Φ_{0bn} and *n* is usually interpreted in terms of barrier height inhomogeneities located at the M/Sc interface [16–20,39–43]. As explained in inhomogeneous SBD model [29], the current conduction is dominated by current flowing through patches exhibiting lower barrier height and a large ideality factor at lower temperatures. When the temperature increases, the electrons gain enough thermal energy to overcome the higher barrier. Hence, the temperature dependence of both the barrier height and the ideality factor are consistent with SBH inhomogeneity. According to the inhomogeneous model [29], a linear correlation between Φ_{0bn} and *n* is expected. Such a correlation is associated with the non-homogenous Schottky contacts. Actually, the experimental values of Φ_{0bn} versus n reported in Fig. 4(a) could be fitted using rather two straight lines with a transition occurring at 160 K. It is worth noting that from the extrapolation of Φ_{0bn}versus *n* plot to the ideal case ($n = 1$), the deduced values at LT (80–160K) and HT (200–400 K) regions of the zero-bias mean value $\overline{\Phi}_{0bn}$ are 0.99 eV and 1.26 eV, respectively. The ideality factor is also analyzed by plotting nk_BT versus k_BT. Such variation is displayed in Fig. 4(b) and shows a linear relationship in the high temperature region (140–300 K) and is parallel to the ideal case ($n = 1$), indicating that the *TE* is the dominant current transport mechanism in our SBD at HT regime.

Table 1
Electrical parameters determined from forward *I–V* characteristics at different temperatures.

Temperature (K)	Current density (A/cm^2)	Ideality factor *n*	Φ_{0bn} (eV)	R_S (Ω)
80	2.6×10^{-21}	2.91	0.41	920
120	6.6×10^{-20}	2.33	0.59	630
160	2.7×10^{-16}	2.01	0.68	425
200	7.7×10^{-14}	1.78	0.76	473
240	1.4×10^{-12}	1.61	0.86	314
280	3.9×10^{-11}	1.5	0.93	306
300	1.8×10^{-10}	1.45	0.96	314
320	10^{-9}	1.42	0.98	306
360	1.9×10^{-8}	1.39	1.02	345
400	4.6×10^{-7}	1.37	1.03	406

According to the *BH*i model, the spatial inhomogeneities of SBH at the interface are interpreted in terms of a Gaussian spatial distribution of SBHs around zero-bias of mean value $\overline{\Phi}_{0bn}$ and with a zero-bias standard deviation σ_{0s} [17–20]. The effective barrier height (Φ_{0bn}) as a function of temperature can be evaluated using:

$$\Phi_{0bn} = \overline{\Phi}_{0bn} - \frac{q^2\sigma_{0s}^2}{2k_B T} \tag{3}$$

The plot of Φ_{0bn}versus $1/2k_BT$ should then result in a straight line with a y-axis intercept equals to $\overline{\Phi}_{0bn}$ and a slope giving the zero-bias standard deviation σ_{0s}. The corresponding plot displayed in Fig. 5 shows a linear behavior but with two different slopes and also two different y-intercepts, with a transition occurring at 160 K. This result may indicate the presence of two Gaussian distributions of SBHs over the Schottky contact area. Accordingly, the deduced values at LT (80–160K) and HT (200–400 K) regions of the zero-bias mean value $\overline{\Phi}_{0bn}$ and the associated zero-bias standard deviation σ_{0s} are ($\overline{\Phi}_{0bn} = 1.32$ eV $\sigma_{0s} = 140$ mV) and ($\overline{\Phi}_{0bn} = 0.96$eV $\sigma_{0s} = 86$ mV), respectively.

In fact, the DGD assumption is supported by the fitting of Φ_{0bn} (T) shown in Fig. 3 using the above values of $\overline{\Phi}_{0bn}$ and σ_{0s}, where the two LT and HT temperature regions are clearly evidenced. Moreover, the respective LT and HT mean value of SBH $\overline{\Phi}_{0bn} = 0.96$ eV and 1.32 eV deduced from Fig. 5 match exactly with the mean SBHs values obtained from Φ_{0bn} versus *n* plot of Fig. 4(a).

The presence of SBH inhomogeneity was also used to explain the deviation from linearity at low temperature in the conventional Richardson plot, namely ln (I_s/T^2) vs. $1/k_BT$. Considering the SBH

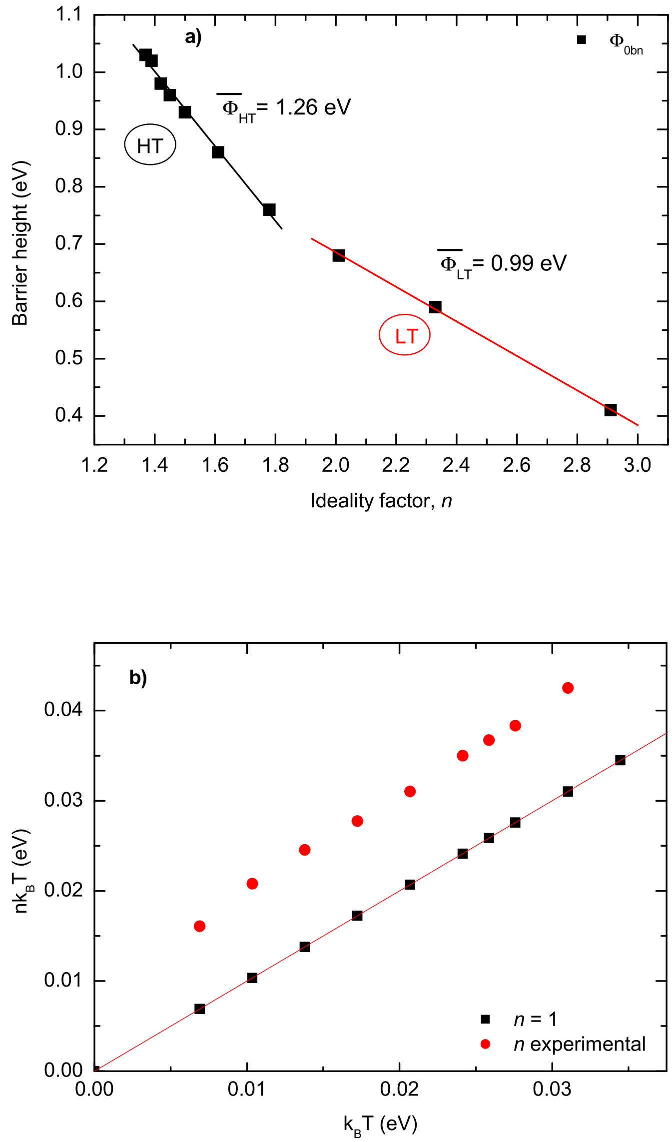

Fig. 4. (a) Effective barrier heights Φ_{0bn} vs. ideality factor n and, (b) nk_BT vs. k_BT plots of Pt/n-GaN SBD at different temperatures.

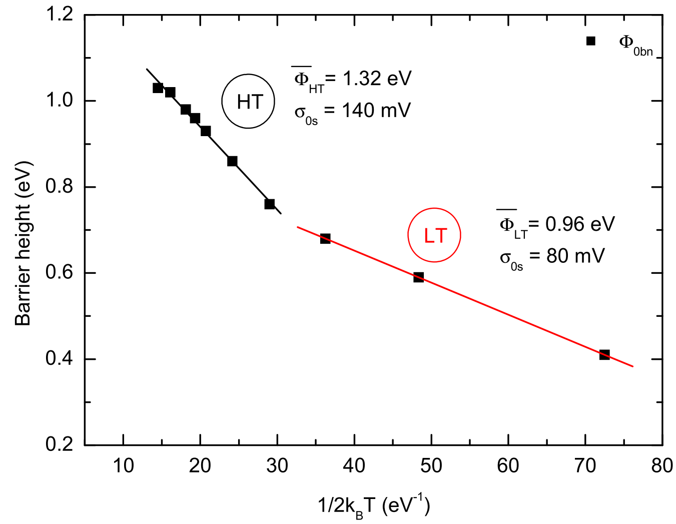

Fig. 5. The effective barrier heights Φ_{0bn} versus$1/2k_BT$ curves of Pt/n-GaN SBD according to the barrier inhomogeneous model [28].

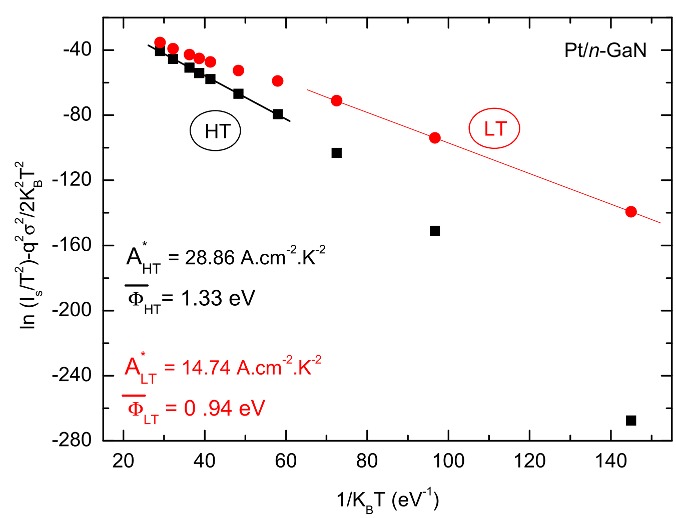

Fig. 6. Modified Richardson plots $\ln\left(\frac{I_S}{T^2}\right)-\left(\frac{q^2\sigma_{0S}^2}{2k_B^2T^2}\right)$ vs. $(1/k_BT)$ associated with both LT and HT regions.

inhomogeneity with double Gaussian distribution of the barrier heights, the modified Richardson plot can be obtained by combining equations (1b) and (3):

$$\ln\left(\frac{I_S}{T^2}\right)-\left(\frac{q^2\sigma_{0s}^2}{2k_B^2T^2}\right)=\ln\left(A^*S\right)-\frac{\overline{\Phi}_{0bn}}{2k_BT} \quad (4)$$

The modified Richardson plots were determined using the two values of σ_{0s} corresponding to the HT and LT regions.

According to equation (4), the modified [ln $\left(\frac{I_S}{T^2}\right)-\left(\frac{q^2\sigma_{0S}^2}{2k_B^2T^2}\right)$ vs. 1/ $2k_BT$] plot should be a straight line with the intercept at the ordinate giving the modified Richardson constant A^*, and the slope giving the zero-bias mean value $\overline{\Phi}_{0bn}$ of SBH (see Fig. 6). The solid squares represent the values corresponding to HT region calculated using σ_{0s} = 140 mV, and the solid circles represent the values related to LT region calculated using σ_{0s} = 86 mV. The result obtained from the analysis of the plots in Fig. 6 provides two sets of deduced values of A^* and $\overline{\Phi}_{0bn}$ corresponding to LT and HT regions (see Table II). The deduced $\overline{\Phi}_{0bn}$ values of 0.94 and 1.33 eV in the two temperature regions match well with the values obtained from the Φ_{0bn} vs. $1/2k_BT$ plots of Fig. 5 (see Table II). The extracted values of Richardson constant at HT region A^*_{HT}

Table 2
Summary of the extracted experimental homogenous SBH and Richardson's constant in the LT and HT regions, along with the results reported in the literature.

System	Theoretical A.cm-^{2}.K-^{2}	A^*_{LT} A. cm-^{2}. K-^{2}	A^*_{HT} A. cm-^{2}. K-^{2}	$\overline{\Phi}_{0bn}$ (eV) (LT)	$\overline{\Phi}_{0bn}$ (eV) (HT)	References
Pt/n-GaN	26.9	14.74	26.86	0.94	1.33	This work
Ru/Pt/ n-GaN		10.29	27.83	0.47	0.99	[22]
Pt/n-GaN		NA	25	NA	1.21	[23]
Pt/n-GaN		NA	35	–	–	[24]
Ni/n-GaN		80	85	0.72	1.42	[14]
Ni/n-GaN		48	29.2	0.73	1.4	[15]

(NA) Not Applicable. I–V measurements have been have performed on M/Sc system at high temperature regime only.

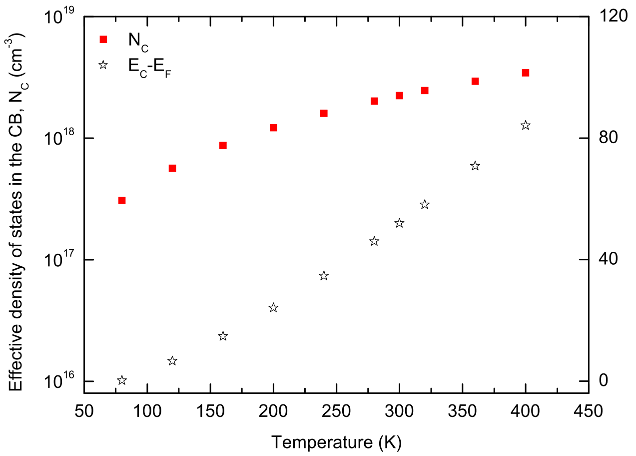

Fig. 7. Effective density of states N_C and the energy difference between the conduction band minimum and Fermi level (E_C-E_F) of Pt/*n*-GaN SBD as a function of temperature.

$= 26.86$ A cm^{-2} K^{-2} is in very good agreement with the theoretical value of 26.9 A cm^{-2} K^{-2}. By contrast its LT counterpart value $A^*_{LT} = 14.74$ A cm^{-2} K^{-2} is much lower.

This discrepancy between the theoretical value of A^* and the experimental extracted value in the low temperature range may indicate that the *TE* is not the major driving conduction mode. We argue that other modes of conduction such as the tunneling current including thermionic field emission (*TFE*) may principally govern the current transport at low temperature regime.

3.2. Investigation of the conduction modes in Pt/n-GaN SBD upon temperature

The *BH*i model associated with Gaussian distribution of SBH shows two distinct temperature regions. Current transport mode in each region (LT and HT) must therefore be considered in the evaluation of inhomogeneities at Pt/*n*-GaN contacts. The high temperature region presents often a behavior in accordance with thermionic conduction mode. In the low temperature region, the *I–V* characteristics could be characterized by a relatively excess of a forward current. This can be attributed to the presence of other dominant current transport modes such as quantum tunneling including thermionic field emission (*TFE*). Indeed, the values of the ideality factor much larger than the unity, the low values of both the barrier height and the Richardson constant obtained in the low temperature range (≤160 K) are usually an indication that the *TE* might no longer be the major conduction mode. Considering the above abnormal features at low temperature regime, we suggest that the *TFE* is the dominant conduction mode as will be evidenced below. From now onwards, the focus will be on the results obtained in the low temperature range (≤160 K).

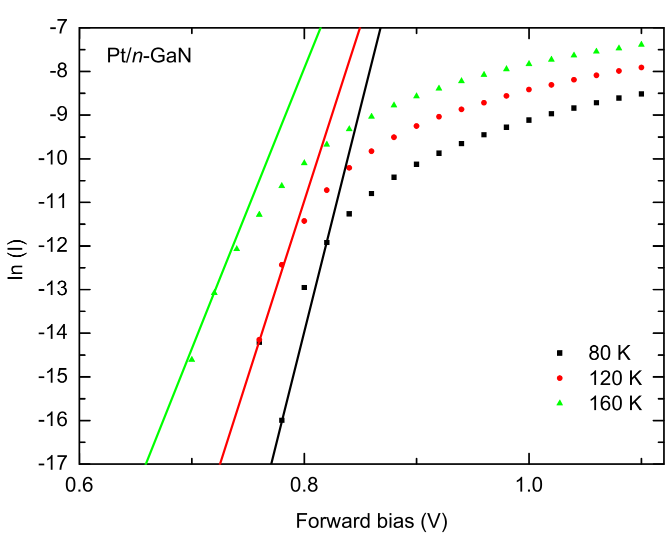

Fig. 8. Experimental forward current curves at the temperatures of 80, 120, and 160 K, and the corresponding fitting curves to *I–V* characteristics according to the *TFE* model.

The *I–V* relation for a Schottky diode based on the *TFE* theory is given by Ref. [44]:

$$I = I_s\left[\exp\left(\frac{q(V - R_s I)}{E_0}\right) - 1\right] \tag{5a}$$

where

$$\mathrm{I_{s,TFE}} = \mathrm{SA^*T}\frac{\sqrt{\pi q E_{00}(\Phi_{bnt}\text{-}V)\text{-}(E_C\text{-}E_F)}}{\mathrm{k_B}\cosh\left(\frac{E_{00}}{k_B T}\right)}\exp\left[\frac{E_C\text{-}E_F}{k_B T}\right]\exp\left[\frac{(E_C\text{-}E_F)+q(V\text{-}\Phi_{bnt})}{E_0}\right] \tag{5b}$$

with

$$E_0 = E_{00}\coth\left[\frac{E_{00}}{k_B T}\right] = n_{tun} k_B T$$

with

$$E_{00} = \hbar \Big/ 2\left[\frac{N_D}{m^*\varepsilon_s}\right]^{1/2}$$

where N_D is the doping density, m^* the effective mass of electron, and ε_s the dielectric constant of GaN.

The depth of Fermi level below the conduction band minimum E_C is expressed as:

$$E_C - E_F = k_B T\ln\left(\frac{N_C}{N_D}\right) \tag{6}$$

where N_C is the effective density of states in the conduction band expressed at given temperature T by:

$$N_C(T) = \frac{2}{h^3}\left(2\pi m_e^* k_B T\right)^{\frac{3}{2}} = 2.5\times 10^{19}\ (\mathrm{cm^{-3}})\left[\frac{m^*}{m_0}\right]^{\frac{3}{2}}\left[\frac{T}{T_0}\right]^{\frac{3}{2}} \tag{7}$$

and T_0 is the room temperature, m_0 the free electron mass; the other entries have their usual meaning.

The doping density N_D obtained from *C–V* measurement for this GaN sample of about 3×10^{17} cm^{-3} is weakly temperature dependent, whereas N_C decreases substantially with decreasing temperature. The variation of both N_C and (E_C-E_F) as a function of temperature is shown in Fig. 7. The Fermi level lies in the vicinity of the conduction band at lower temperature, with a maximum value of 14.7 meV at 160 K. Therefore, this GaN can be considered as a degenerate semiconductor likewise heavily doped. This result supports further the assumption that the current transport mode across SBD is dominated by the quantum tunneling transport [45]. Indeed, the *I–V* curves at temperature below 160 K are well fitted using Eqs. (5a) and (5b) based on the *TFE* model as shown in Fig. 8. The extracted characteristics parameters from curves fitting using Eqs. (5a) and (5b), namely n_{tun}, Φ_{bnt}, and E_C-E_F based on *TFE* model are reported in Table III.

The above results provide a good evidence that the existence of the DGD, usually observed in M/Sc contacts can be well interpreted in terms of two different conduction modes: (*i*) a dominant thermionic emission mode at high temperature regime, and (*ii*) a dominant tunneling thermionic field emission at low temperature regime.

Table 3
Summary of the fitting parameters used for *I–V* characteristics of Pt/*n*-GaN SBD in *TFE* mode.

Temperature (K)	Φ_{bnt} (eV)	n_{tun}	E_C-E_F (meV)
80	1.01	1.38	0.18
120	1.04	1.17	6.56
160	1.06	1.01	14.70

4. Conclusion

In this work, we have investigated the temperature dependence of the forward current-voltage characteristics of Pt/*n*-GaN Schottky contacts in order to explain the abnormal behavior usually observed associated with the double Gaussian distribution of the SBH within the *TE* model. Such abnormal SBH distribution is associated with two main regions usually low (80–160K) and high (200–400) temperature range. Numerous works show incoherent values of SBH, ideality factor and Richardson constant at low temperature region. We demonstrate in this work that the above abnormal features observed at low temperature are correlated with the use of the *TE* conduction mode. Indeed, the *TFE* model has been utilized to interpret properly the low temperature regime. The deviation from the *TE* current at low temperature is thus explained by the occurrence of degeneracy-like of GaN and the whole *I–V* characteristics at low temperature region are well fitted within the *TFE* model.

It is therefore of paramount importance to consider tunneling conduction mode at low temperature regime when investigating the barrier height inhomogeneities in devices involving GaN-based Schottky contacts.

CRediT authorship contribution statement

Mohammed Mamor: Conceptualization, Data curation, Formal analysis, Investigation, Methodology, Writing – original draft, Writing – review & editing. **Khalid Bouziane:** Writing – original draft, Conceptualization, Data curation, Formal analysis, Investigation, Methodology, Writing – review & editing. **Hind Chakir:** Conceptualization, Data curation, Formal analysis, Investigation, Methodology, Writing – original draft, Writing – review & editing. **Pierre Ruterana:** Writing – review & editing, Writing – original draft, Conceptualization, Data curation, Formal analysis, Investigation, Methodology.

Declaration of competing interest

The authors declare that they have no known competing financial interests or personal relationships that could have appeared to influence the work reported in this paper.

Data availability

Data will be made available on request.

References

[1] K.J. Chen, O. Häberlen, A. Lidow, C.L. Tsai, T. Ueda, Y. Uemoto, Y. Wu, GaN-on-Si power technology: devices and applications, IEEE Trans. Electron. Dev. 64 (2017) 779.
[2] S. Singh, T. Chaudhary, G. Khanna, Recent advancements in wide band semiconductors (SiC and GaN) technology for future devices, Silicon 14 (2022) 5793.
[3] C. Lee, W. Lin, Y. Lee, J. Huang, Characterizations of enhancement-mode double heterostructure GaN HEMTs with gate field plates, IEEE Trans. Electron. Dev. 65 (2018) 488.
[4] S.J. Pearton, F. Ren, GaN electronics, Adv. Mater. 12 (2000) 1571.
[5] T.H. Yang, J. Brown, K. Fu, J. Zhou, K. Hatch, C. Yang, J. Montes, X. Qi, H. Fu, R. J. Nemanich, Y. Zhao, AlGaN/GaN metal–insulator semiconductor high electron mobility transistors (MISHEMTs) using plasma deposited BN as gate dielectric, Appl. Phys. Lett. 118 (2021) 072102.
[6] S. Nakamura, G. Fasol, The Blue Laser Diode, Springer Verlag, 1997.
[7] N.K.R. Nallabala, S. Godavarthi, V.K. Kummara, M.K. Kesarla, D. Saha, H. S. Akkera, G.K. Guntupalli, S. Kumar, S.V.P. Vattikuti, Structural, optical and photo response characteristics of metal-insulator-semiconductor (MIS) type Au/Ni/CeO_2/GaN Schottky barrier ultraviolet photodetector, Mater. Sci. Semicond. Process. 117 (2020) 105190.
[8] V. Manjunath, N.K.R. Nallabala, C. Yuvaraj, C. Kukkambakam, V.K. Kummara, S. Kumar, S. Sharma, M.V. Lakshmaiah, V.R.M. Reddy, Statistical analysis of current–voltage characteristics in Au/Ta_2O_5/n-GaN Schottky barrier heterojunction using different methods, Appl. Phys. A 127 (2021) 46.
[9] N.K.R. Nallabala, S. Godavarthi, V.K. Kummara, M.K. Kesarla, C. Yuvaraj, S. Kumar, N. Ravi, G.K. Guntupalli, S.A.K. Jilani, S.V.P. Vattikuti, High performance, self-powered and thermally stable 200–750 nm spectral responsive gallium nitride (GaN) based broadband photodetectors, Sol. Energy Mater. Sol. Cells 225 (2021) 111033.
[10] B. Shankar, A. Soni, M. Shrivastava, Electro-thermo-mechanical reliability of recessed barrier AlGaN/GaN Schottky diodes under pulse switching conditions, IEEE Trans. Electron. Dev. 67 (2020) 2044.
[11] N.K.R. Nallabala, S.V.P. Vattikuti, V.K. Verma, V.R. Singh, S. Alhammadi, V. K. Kummara, V. Manjunath, M. Dhanalakshm, V.R.M. Reddy, Highly sensitive and cost-effective metal-semiconductor-metal asymmetric type Schottky metallization based ultraviolet photodetecting sensors fabricated on n-type GaN, Mater. Sci. Semicond. Process. 138 (2022) 106297.
[12] J. Koba, J. Koike, Low contact resistivity of metal/n-GaN by the reduction of gap states with an epitaxially grown GaO_x insulating layer, AIP Adv. 12 (2022) 085302.
[13] N.K.R. Nallabala, V.R.M. Reddy, V.R. Singh, K.R. Bakash, S. Kumar, D. Saha, V. Mahendran, V.K. Kummara, G.K. Guntupalli, S.V.P. Vattikuti, Enhanced photoresponse performance in GaN based symmetric type MSM ultraviolet-A and MIS ultraviolet-A to C photodetectors, Sensor. Actuat. A-Phys. 339 (2022) 113502.
[14] L. Huang, F. Qin, S. Li, D. Wang, Effects of surface properties on barrier height and barrier inhomogeneities of platinum contacts to n-type 4H-SiC, Appl. Phys. Lett. 103 (2013) 033520.
[15] S. Shivaraman, L.H. Herman, F. Rana, J. Park, M.G. Spencer, Schottky barrier inhomogeneities at the interface of few layer epitaxial graphene and silicon carbide, Appl. Phys. Lett. 100 (2012) 183112.
[16] L. Huang, D. Wang, Barrier inhomogeneities and electronic transport of Pt contacts to relatively highly doped n-type 4H SiC, J. Appl. Phys. 117 (2015) 204503.
[17] T. Tunç, Ş. Altındal, İ. Uslu, İ. Dökme, H. Uslu, Temperature dependent current–voltage (I–V) characteristics of Au/n-Si (1 1 1) Schottky barrier diodes with PVA(Ni,Zn-doped) interfacial layer, Mater. Sci. Semicond. Process. 14 (2011) 139.
[18] N. Yıldırım, K. Ejderha, A. Turut, On the temperature-dependent experimental I-V and C-V data of Ni/n-GaN Schottky contacts, J. Appl. Phys. 108 (2010) 114506.
[19] E. Özavcı, S. Demirezen, U. Aydemir, Ş. Altındal, A detailed study on current–voltage characteristics of Au/n-GaAs in wide temperature range, Sensor. Actuat. A-Phys. 194 (2013) 259.
[20] M. Mamor, Interface gap states and Schottky barrier inhomogeneity at metal/*n*-type GaN Schottky contacts, J. Phys. Condens. Matter 21 (2009) 335802.
[21] A. Turut, On current-voltage and capacitance-voltage characteristics of metal-semiconductor contacts metal-semiconductor contacts, Turk. J. Phys. 44 (2020) 302.
[22] A. Kumar, S. Vinayak, R. Singh, Micro-structural and temperature dependent electrical characterization of Ni/GaN Schottky barrier diodes, Curr. Appl. Phys. 13 (2013) 1137.
[23] A. Kaya, S. Demirezen, H. Tecimer, Ş. Altındal, Temperature and voltage effect on barrier height and ideality factor in Au/PVC + TCNQ/p-Si structures, Adv. Polym. Technol. 33 (2014) 21442.
[24] A.F. Özdemir, Z. Kotan, D.A. Aldemir, S. Altındal, The effects of the temperature on I-V and C-V characteristics of Al/P2ClAn(C_2H_5COOH)/p-Si/Al structure, Eur. Phys. J. Appl. Phys. 46 (2009) 2042.
[25] F.M. Coşkun, O. Polat, M. Coşkun, A. Turut, M. Caglar, Z. Durmus, H. Efeoğlu, Temperature dependent current transport mechanism in osmium-doped perovskite yttrium manganite-based heterojunctions, J. Appl. Phys. 125 (2019) 214104.
[26] Ç.Ş. Güçlü, A.F. Özdemir, A. Karabulut, A. Kökce, Ş. Altındal, Investigation of temperature dependent negative capacitance in the forward bias C-V characteristics of (Au/Ti)/Al_2O_3/n-GaAs Schottky barrier diodes (SBDs), Mater. Sci. Semicond. Process. 89 (2019) 26.
[27] İ. Taşçıoğlu, G. Pirgholi-Givi, S. AltındalYerişkin, Y. Azizian-Kalandaragh, Examination on the current conduction mechanisms of Au/n-Si diodes with ZnO–PVP and ZnO/Ag_2WO_4 –PVP interfacial layers, J. Sol. Gel Sci. Technol. 107 (2023) 536.
[28] J.H. Werner, H.H. Güttler, Barrier inhomogeneities at Schottky contacts, J. Appl. Phys. 69 (1991) 1522.
[29] R.T. Tung, Electron transport at metal-semiconductor interfaces: general theory, Phys. Rev. B 45 (1992) 13509.
[30] P. Song, R.L. Van Meirhaeghe, W.H. Laflere, F. Cardon, On the difference in apparent barrier height as obtained from capacitance-voltage and current-voltage-temperature measurements on Al/p-InP Schottky barriers, Solid State Electron. 29 (1986) 633.
[31] A. Itoh, T. Kimoto, H. Matsunami, High performance of high-voltage 4H-SiC Schottky barrier diodes, IEEE Trans. Electron. Dev. 16 (1995) 280.
[32] F. Roccaforte, F.L. Via, V. Rainer, R. Pierobon, E. Zanoni, Richardson's constant in inhomogeneous silicon carbide Schottky contacts, J. Appl. Phys. 93 (2003) 9137.
[33] N.N.K. Reddy, V. Reddy, Barrier characteristics of Pt/Ru Schottky contacts on *n*-type GaN based on *I–V–T* and *C–V–T* measurements, Bull. Mater. Sci. 35 (2012) 53.

[34] F. Iucolano, F. Roccaforte, F. Giannazzo, V. Raineri, Barrier inhomogeneity and electrical properties of Pt/GaN Schottky contacts, J. Appl. Phys. 102 (2007) 113701.
[35] Y. Zhou, D. Wang, C. Ahyi, C.-C. Tin, J. Williams, M. Park, N.M. Williams, A. Hanser, E.A. Preble, Temperature-dependent electrical characteristics of bulk GaN Schottky rectifier, J. Appl. Phys. 101 (2007) 024506.
[36] A.M. Witowski, K. Pakuła, J.M. Baranowski, M.L. Sadowski, P. Wyder, Electron effective mass in hexagonal GaN, Appl. Phys. Lett. 75 (1999) 4154.
[37] E.H. Rhoderick, R.H. Williams, Metal-Semiconductor Contacts, Clarendon Press, Oxford, UK: Oxford Science, 1988, p. 38, 2nd ed.
[38] J.H. Werner, Schottky barrier and pn-junction *I/V* plots — small signal evaluation, Appl. Phys. A 47 (1988) 291.
[39] M. Mamor, K. Bouziane, A. Tirbiyine, Barrier inhomogeneities in titanium Schottky contacts formed on argon plasma etched p-type $Si_{0.95}Ge_{0.05}$, J. Mater. Sci. Mater. Electron. 25 (2014) 1527.
[40] N. Yıldırım, A. Turut, V. Turut, The theoretical and experimental study on double-Gaussian distribution in inhomogeneous barrier-height Schottky contacts, Microelectron. Eng. 87 (2010) 2225.
[41] S. Chand, S. Bala, Analysis of current–voltage characteristics of inhomogeneous Schottky diodes at low temperatures, Appl. Surf. Sci. 252 (2005) 358.
[42] M. Mamor, K. Bouziane, A. Tirbitine, H. Alhamrashdi, On the electrical characteristics of Au/n-type GaAs Schottky diode, Superlattice. Microst. 72 (2014) 344.
[43] N. Yıldırım, A. Turut, A theoretical analysis together with experimental data of inhomogeneous Schottky barrier diodes, Microelectron. Eng. 86 (2009) 2270.
[44] F.H. Padovani, R. Stratton, Field and thermionic-field emission in Schottky barriers, Solid State Electron. 9 (1966) 695.
[45] D.K. Schroder, Semiconductor Material and Device Characterization, Wiley Interscience, Hoboken, NJ, 2006, p. 160.